Lusernaite-(Y), Y4Al(CO3)2(OH,F)11·6H2O, a new mineral species from Luserna Valley, Piedmont, Italy: Description and crystal structure

Biagioni C; Bonaccorsi E; Cámara F; Cadoni M; Ciriotti ME; Bersani D; Kolitsch U. Lusernaite-(Y), Y4Al(CO3)2(OH,F)11·6H2O, a new mineral species from Luserna Valley, Piedmont, Italy: Description and crystal structure. AMERICAN MINERALOGIST. 98 pp: 1322-1329. DOI: 10.2138/am.2013.4366

Lusernaite-(Y), $Y_4Al(CO_3)_2(OH,F)_{11}\cdot 6H_2O$, a new mineral species from Luserna Valley, Piedmont, Italy: description and crystal structure

CRISTIAN BIAGIONI[1], ELENA BONACCORSI[1], FERNANDO CÁMARA[2,3], MARCELLA CADONI[2,3], MARCO E. CIRIOTTI[4], DANILO BERSANI[5], UWE KOLITSCH[6,7]

[1] *Dipartimento di Scienze della Terra, Università di Pisa, Via S. Maria 53, I-56126 Pisa, Italy*
[2] *Dipartimento di Scienze della Terra, Università di Torino, Via Valperga Caluso 35, I-10125 Torino, Italy*
[3] *CrisDi, Interdepartmental Centre for the Research and Development of Crystallography, Via P. Giuria 5, I-10125, Torino, Italy*
[4] *Associazione Micro-mineralogica Italiana, Via San Pietro 55, I-10073 Devesi/Cirié, Torino, Italy*
[5] *Dipartimento di Fisica, Università di Parma, Viale G.P. Usberti 7/a, I-43100 Parma, Italy*
[6] *Mineralogisch-Petrographische Abt., Naturhistorisches Museum, Burgring 7, 1010 Wien, Austria*
[7] *Institut für Mineralogie und Kristallographie, Geozentrum, Universität Wien, Althanstraße 14, 1090 Wien, Austria*

**e-mail address: biagioni@dst.unipi.it*

ABSTRACT

The new mineral species lusernaite-(Y), ideally $Y_4Al(CO_3)_2(OH,F)_{11}\cdot 6H_2O$, has been discovered in small fractures of the "Luserna Stone", a leucocratic orthogneiss belonging to the Dora-Maira massif, Western Alps, Italy. It occurs as colorless, thin platelets, with white streak and mica-like pearly luster, elongated along [100] and flattened on {010}, arranged in radiating aggregates. Lusernaite-(Y) is associated with aeschynite-(Y), albite, "chlorite", hematite, pyrite, quartz, and titanite. Lusernaite-(Y) has a perfect cleavage on {010} and a less marked one probably on {001}. Its calculated density is 2.810 $g\cdot cm^{-3}$. In plane polarized light, it is transparent, with parallel extinction and positive elongation. Owing to the crystal morphology, only two refractive indices could be measured, corresponding to 1.576(2)-1.578(2) along [100] and 1.566(2) along [001].

Lusernaite-(Y) is orthorhombic, space group *Pmna*, with *a* 7.8412(3), *b* 11.0313(5), *c* 11.3870(4) Å, *V* 984.96(7) $Å^3$, *Z* = 2. Main diffraction lines of the X-ray powder diffraction pattern are [*d* in Å, (*I*), (*hkl*)]: 11.02 (100) (010), 7.90 (49) (011), 5.66 (25) (002), 5.06 (24) (012), 4.258 (33) (112), 3.195 (27) (220), 3.095 (21) (212). Raman spectroscopy confirmed the presence of CO_3 groups (sharp peak at 1096 cm^{-1}); due to the very strong luminescence, the bands of the OH and H_2O groups could not be seen.

Chemical analyses by electron microprobe gave (wt.%) Al_2O_3 6.11, Y_2O_3 43.52, La_2O_3 0.02, Ce_2O_3 0.04, Nd_2O_3 0.03, Sm_2O_3 0.16, Gd_2O_3 1.39, Dy_2O_3 3.46, Er_2O_3 3.15, Yb_2O_3 2.09, CaO 0.33, PbO 0.37, H_2O 22.74, CO_2 9.94, F 1.40, O ≡ F -0.59, sum 94.16; H_2O and CO_2 were determined from structure refinement. The empirical formula by assuming the presence of two $(CO_3)^{2-}$ groups, eleven $(OH,F)^-$ anions, and six H_2O molecules, in agreement with micro-Raman and structural results, is $(Y_{3.41}Dy_{0.16}Er_{0.15}Yb_{0.09}Gd_{0.07}Ca_{0.06}Pb_{0.02}Sm_{0.01})_{\Sigma 3.97}Al_{1.06}(CO_3)_{2.00}(OH_{10.34}F_{0.66})\cdot 6H_2O$.

The crystal structure was solved by direct methods and refined on the basis of 840 observed reflections to R_1 = 6.8%. In the structure of lusernaite-(Y), yttrium and *REE* cations occupy two distinct sites, Y1 and Y2, both in eight-fold coordination. The structure is built by layers parallel to (010), formed by chains of edge-sharing Y-centered polyhedra (Y1), which run along [100], and are connected along **c** through Al-centered octahedra. These chains are decorated on one side by corner-sharing chains of Y-centered polyhedra (Y2), and on the other side by CO_3 groups. Along [001] the decorated chains alternate their polarity.

Lusernaite-(Y), named after the type locality, the Luserna Valley, shows a new kind of structure among the natural carbonates of *REE*. Its origin is related to the circulation of hydrothermal solutions during the late-stage Alpine tectono-metamorphic events.

Key words: lusernaite-(Y), new mineral species, carbonate, yttrium, crystal structure, Luserna stone, Piedmont, Italy.

INTRODUCTION

The "Luserna stone", a leucocratic orthogneiss, has been quarried since the Middle Age and it is an important historical stone for its widespread occurrence and use in historical monuments. The first publications about this stone date back to the beginning of the 19th Century, with the studies of Barelli (1835) and De Bartolomeis (1847), focused on the technological and economic importance of the quarrying activities. The first scientific work can be considered that of Gastaldi (1874), who tentatively reconstructed the lithostratigraphic setting of the "Luserna stone". Since then, a large number of studies about this stone have been published (Sandrone, 2001). Surprisingly, only recently the mineralogical peculiarities of this formation have been investigated. Vaccio (2002), Piccoli *et al*. (2007), and Finello *et al*. (2007) described the minerals occurring in late-stage fractures in the "Luserna stone", reporting more than 40 different mineral species. A large number of *REE* and Y phases were listed by the latter authors, including aeschynite-(Y), allanite-(Ce), aluminocerite-(Ce), cerite-(Ce), fergusonite-(Y), hellandite-(Y), kainosite-(Y), monazite-(Ce), synchysite-(Ce), xenotime-(Y), and probably polycrase-(Y). In addition, some unidentified minerals have been described; among these, the mineral UK01 which corresponds to the new mineral species lusernaite-(Y).

The new species and its name have been approved by the IMA-CNMNC (no. 2011-108). It is named after the type locality, the Luserna Valley (Piedmont, Italy); the Levinson suffix (Bayliss & Levinson, 1988) indicates the dominance of Y among Y and *REE*. The type material is deposited in the mineralogical collections of the Museo di Storia Naturale e del Territorio, University of Pisa, Via Roma 79, Calci (Pisa, Italy) under the catalog number 19445. A cotype specimen is kept in the mineralogical collections of the Museo Regionale di Scienze Naturali, Via Giovanni Giolitti 36, Torino (Italy), with catalog number M/15901.

GEOLOGICAL SETTING AND MINERAL OCCURRENCE

The "Luserna stone" refers to a heterogeneous series of leucocratic gneisses (characterized by a micro-*Augen* texture and grey-greenish or locally pale blue color) and phengitic schists, outcropping in an area 50 km^2 wide in the Cottian Alps, at the border of the provinces of Torino and Cuneo. This complex forms a flat body structurally located at the top of the Dora-Maira massif, the southernmost of the so-called Internal Crystalline Massif of the Western Alps (Bussy & Cadoppi, 1996).

Whereas Vialon (1966) interpreted the "Luserna stone" as a metamorphosed volcano-sedimentary sequence, other authors proposed a granitic origin on the basis of petrographic and geochemical data (Cadoppi, 1990; Bussy & Cadoppi, 1996; Sandrone *et al*., 2004). The age of this complex is still unknown; U-Pb dating on zircon indicates that most of the dated metagranites belonging to the Dora-Maira massif were emplaced during the Upper Carboniferous, in relation with the Variscan orogeny (Bussy & Cadoppi, 1996).

Mineral assemblages and phase chemistry suggest an Alpine metamorphic evolution characterized by an early eclogite-*facies* stage at pressures between 1.4 and 2.5 GPa for 550 ± 50°C; this stage was overprinted by a greenschist-*facies* metamorphism due to the exhumation of all the European basement units at 35-40 My (Scaillet *et al*., 1992).

Mineralogically, the "Luserna stone" is composed of quartz (30-45 vol.%), K-feldspar (10-25 vol.%), albite (15-25 vol.%), "phengite" (10-20 vol.%), and subordinate "biotite", "chlorite", and epidote-group minerals. Common accessories are opaque phases, titanite, "apatite", and zircon; locally, "tourmaline", carbonates, "axinite", and fluorite are also present (Sandrone *et al*., 2004).

Finello *et al*. (2007) described two kinds of mineral occurrence: *i*) in small fractures, normal to the main field foliation, probably related to the late-stage tectonic events; and *ii*) in small aplite dykes, parallel to the main foliation. Lusernaite-(Y) was found only in the first kind of occurrence.

Lusernaite-(Y) was found in the Seccarezze quarries, Luserna San Giovanni, Torino, Piedmont, Italy. The first find of lusernaite-(Y) dates back to the 1991, when a mineral collector, G. Finello, found two specimens of a phase that proved to be a possible new mineral species and was described as UK01 (UKGFN009Mugniv) by Finello *et al*. (2007); a new find of better quality was made in 2006 by the mineral collectors B. Marello and C. Alciati. Other findings of this rare mineral were done in October 2009 (about 15 specimens) and in April-May 2010 (eight collected specimens). The new findings allowed determining the mineral and its approval as a new species. Finally, a last finding of lusernaite-(Y) occurred in March 2012, as radial aggregates of well-developed tabular crystals, in one case associated with calcite.

The crystallization of lusernaite-(Y) is probably related to the circulation of hydrothermal fluids in late-stage fractures during the Tertiary Alpine tectono-metamorphic events.

MINERALOGICAL CHARACTERIZATION

Appearance and physical properties

Lusernaite-(Y) occurs as thin platelets, up to 1 mm in size, with an indistinct, roughly six-sided outline. Crystals are elongated along **a** and flattened on {010} and are arranged in radiating aggregates (Fig. 1). Associated minerals are aeschynite-(Y), albite, "chlorite", hematite, pyrite, quartz, and titanite.

Lusernaite-(Y) is colorless, with a white streak and a mica-like pearly luster. In plane polarized light, it is transparent. Between crossed polars, the mineral shows parallel extinction, with a positive elongation parallel to [100]. Birefringence is weak. Refractive indices were measured in white light using the Becke line method; due to the crystal morphology, only the two refractive indices laying within the (010) plane could be measured. The measured refractive indices are α' 1.566(2) and γ' 1.576(2)-1.578(2). The mean refractive index *n* of lusernaite-(Y), calculated using the Gladstone-Dale relationship (Mandarino, 1979, 1981), using the empirical formula obtained assuming the presence of stoichiometric CO_2 and H_2O (see below), is 1.588. The difference between the measured values and the calculated mean refractive index may be ascribed to chemical variations; for example, the greater the fluorine content, the lower is the mean refractive index of lusernaite-(Y). In addition, other possible ionic substitution in the cation sites (*e.g*. differences in the relative abundance of *REE* and Y) may be invoked.

Density was not measured, due to the small crystal size and the difficulty in observing the mineral in the heavy liquids; the calculated density, based on the empirical formula used for the calculation of the mean refractive index, is 2.810 $g \cdot cm^{-3}$.

Lusernaite-(Y) is brittle, with a perfect {010} cleavage; another cleavage (probably on {001}) was observed normal to the crystal elongation. Owing to the difficulty in preparing a polished surface and to the softness of the mineral, a reliable value of hardness could not be measured.

CHEMICAL AND SPECTROSCOPIC DATA

Chemical Data

Preliminary qualitative chemical analysis by energy-dispersive spectroscopy was performed using a Phillips LX30 SEM, equipped with an EDAX DX4 system. It indicated that the only elements with $Z > 9$ occurring in lusernaite-(Y) are Y, Al, F, and minor Dy, Gd, and Er.

Quantitative chemical data were collected using a JEOL JXA-8200 electron-microprobe, using an acceleration voltage of 15 kV and a beam current of 5 nA. The beam size was set to 15 μm in order to prevent (or limit) the deterioration of the crystal of lusernaite-(Y); notwithstanding this, some surficial damage of the analyzed crystals was observed. Standards were (element, emission line): anorthite (Al*K*α, Ca*K*α), synthetic YPO_4 (Y*L*α), synthetic *REE*PO_4 set (La*L*α, Ce*L*α, Dy*L*α, Nd*L*α, Er*L*α, Yb*L*α, Gd*L*α, Sm*L*α), galena (Pb*M*α), synthetic $RbMnF_3$ (F *K*α). Concentrations of the *REE* were corrected for overlaps. Fluorine concentration was measured on the basis of the F*K*α peak height; consequently, its measure is probably not accurate, owing to the problems associated with F*K*α peak shape and breadth:height variability (*e.g*. Solberg, 1982; Raudsepp, 1995; Ottolini *et al*., 2000).

Table 1 gives the weight concentrations obtained on a polished fragment of lusernaite-(Y). The reported H_2O and CO_2 contents were estimated, in agreement with the results of the crystal structure study, showing the presence of two $(CO_3)^{2-}$ groups, eleven $(OH,F)^-$ anions, and six H_2O groups per formula unit (*pfu*). The low total, *i.e*. 94.16 wt.%, could be attributed to the superficial damage of the sample and to the difficulty in preparing a good quality polished surface.

The empirical formula of lusernaite-(Y), based on 23 anions *pfu*, is $(Y_{3.41}Dy_{0.16}Er_{0.15}Yb_{0.09}Gd_{0.07}Ca_{0.06}Pb_{0.02}Sm_{0.01})_{\Sigma 3.97}Al_{1.06}(CO_3)_{2.00}(OH_{10.34}F_{0.66})\cdot 6H_2O$. The empirical formula simplifies to $Y_4Al(CO_3)_2(OH)_{11}\cdot 6H_2O$, which requires (wt%) Y_2O_3 56.61, Al_2O_3 6.39, CO_2 11.03, H_2O 25.97, total 100.00.

Lusernaite-(Y) is slowly soluble in dilute 1:10 HCl, with the development of small gas bubbles, in agreement with the occurrence of carbonate groups in its structure.

Micro-Raman spectroscopy

Unpolarized micro-Raman spectra (Fig. 2) were obtained on an unpolished crystal of lusernaite-(Y) in nearly back-scattered geometry, with a Jobin-Yvon Horiba "Labram" apparatus, equipped with a motorized *x-y* stage and an Olympus microscope with a 50× objective. The 632.8 nm line of a He-Ne laser and the 473.1 nm line of a Nd:YAG laser were used. The minimum lateral and depth resolution were set to a few micrometers. The system was calibrated using the 520.6 cm^{-1} Raman peak of silicon before each experimental session. Spectra were collected through multiple acquisitions with single counting times ranging between 20 and 180 s. Both Raman spectra obtained with 473.1 and 632.8 nm excitation lines are dominated by strong luminescence features, in the form of many groups of sharp bands, superimposed on a broad band centered at about 570 nm. The only features ascribable to a Raman band is the sharp peak at 1096 cm^{-1}, confirming the presence of CO_3^{2-} groups in the structure.

The main luminescence peaks are located in the region between 560 and 590 nm; the strongest ones are at 573, 576, and 582 nm. Other weaker groups of luminescence bands are visible in the regions around 488 and 752 nm (using the 473.1 nm excitation) and 660 nm (using the 632.8 nm line). Dy^{3+} impurities could be the cause of these luminescence bands, except the broad ones (Gaft

et al., 2005); this observation agrees with the fact that Dy^{3+} is the main substituent of Y^{3+}, as shown by EPMA data. Due to the strong luminescence, even in the region of the bending and stretching of O-H bonds, no detectable Raman signals could be collected.

X-RAY CRYSTALLOGRAPHY AND CRYSTAL STRUCTURE DETERMINATION

The powder X-ray diffraction pattern of lusernaite-(Y) was obtained using a 114.6 mm Gandolfi camera and Ni-filtered Cu*K*α radiation (Table 2). Indexing of the reflections was based on a calculated powder pattern obtained by the structural model described below, using the software POWDERCELL (Kraus & Nolze, 2000). The unit-cell parameters refined from the powder data with the software UNIT CELL (Holland & Redfern, 1997), on the basis of 24 univocally indexed reflections, are: *a* 7.839(2), *b* 11.023(2), *c* 11.383(2) Å, *V* 983.6(2) $Å^3$.

Preliminary Weissenberg photographs were obtained using a small crystal of lusernaite-(Y) and allowed the morphological orientation of the crystal.

Single-crystal X-ray diffraction data were collected using an Oxford Gemini R Ultra diffractometer equipped with a CCD area detector at CrisDi (Interdepartmental Centre for the Research and Development of Crystallography, Torino, Italy). Graphite-monochromatized Mo*K*α radiation was used. Crystal data and experimental details are reported in Table 3. Some 763 frames were collected in 1.0° slices between ω angles 3.57° and 33.49°. The exposure time was 130 s per frame. Data were integrated and corrected for Lorentz and polarization, background effects, and absorption, using the package CRYSALIS^{Pro} (Oxford Diffraction, 2007a, b). Refinement of the unit-cell parameters was based on all measured reflections with $I > 200\sigma(I)$. At room temperature, the unit-cell is *a* 7.8412(3), *b* 11.0313(5), *c* 11.3870(4) Å, *V* 984.96(7) $Å^3$, space group *Pmna*, *Z* = 2. The *a*:*b*:*c* ratio is 0.711:1:1.032. A total of 1081 independent reflections were collected and the structure was solved and refined by means of the SHELX set of programs (Sheldrick, 2008).

After having located the Y and Al atoms, the structure was completed through successive difference-Fourier maps. The latter showed the presence of two maxima around one of the two Y-centered sites, *i.e*. Y1, at 0.80 and 0.98 Å, respectively. On the basis of chemical data, these residuals were attributed to Pb, lowering significantly the *R* values.

The refined occupancies of the Y1, Y2, Pb1a, and P1b sites were $Y_{0.370(8)}Er_{0.116(8)}$, $Y_{0.457(7)}Dy_{0.043(7)}$, $Pb_{0.007(1)}$, and $Pb_{0.007(1)}$, respectively. This indicates that the other *REE* measured by EPMA prefer to occupy Y1 and Y2 sites. The two refined Pb occupancies would equal to a Pb content of 0.06 *apfu*, a value which is higher than the measured value of 0.015 Pb *pfu*. Thus, it may also be possible that some of the measured *REE*, which have ionic radii fairly different from that of Y^{3+} (*e.g*. Gd^{3+}, Yb^{3+}), may reside in these satellite positions.

Furthermore, some unacceptably short Pb-φ distances are observed, *e.g*. Pb1a – O2 1.83(3)Å and Pb1b – O6 2.03(1) Å, and the actual coordination of these split sites cannot be assessed. The total refined site scattering value at the Y1+Y2 sites is 177.1 e^-, to be compared with 167.9 e^- obtained from the chemical data. Two hydrogen positions were located in the difference-Fourier maps; these hydrogen atoms were added to the model but their coordinates and isotropic displacement parameters were not refined. Examination of the bond-valence balance and the hydrogen bonds suggested that two O sites, namely O4 and O5, are possible F-bearing sites. A lower *R* value was achieved by introducing fluorine at the O4 site, which was consequently renamed F4. The O:F ratio in the F4 site was fixed taking into account the EPMA data.

Refinement converged to R_1 = 6.81% for 840 observed reflections and 89 parameters. The largest peak and hole in the final difference Fourier map are 2.67 and -1.09 *e* $Å^{-3}$, respectively. Tables 4 and 5 report the atomic coordinates and displacement parameters, and selected bond distances, respectively.

DESCRIPTION AND DISCUSSION OF THE STRUCTURE

General features and cation coordination

The crystal structure of lusernaite-(Y) (Fig. 3) is layered on (010); layering is a common feature of (Y,*REE*) carbonates (Grice *et al*., 1994; Grice *et al*., 2007). In lusernaite-(Y) only one kind of layer occurs; it is composed by two independent Y-centered polyhedra, one Al-centered octahedron, one C-centered triangle, six anion positions, and three H_2O groups.

The two Y-centered sites, namely Y1 and Y2, are eight-fold coordinated. The average Y-φ bond-lengths are 2.387 and 2.351 Å for Y1 and Y2 sites, respectively, with single values ranging from 2.267 (Y2-O4 bond) to 2.485 (Y1-O5 bond) Å. Probably Pb occupies two sub-positions, owing to its stereochemical activity; similar behavior has been observed for lead replacing potassium in synthetic $Pb_2(Pb,K)_4[Si_8O_{20}]O$ (Moore *et al*., 1985) and lead replacing barium in hyalotekite (Moore *et al*., 1982; Christy *et al*., 1998). Aluminum is octahedrally coordinated, with an average bond-length of 1.898 Å. The planar carbonate groups (CO_3) are inclined with respect to the overall structural layering; they are attached through corner-sharing to two Y1-centered polyhedra.

The (010) layer is built by chains of edge-sharing Y-centered polyhedra (Y1 site), which run along [100], and are connected along [001] through Al-centered octahedra. These chains are decorated on one side by corner-sharing chains of Y-centered polyhedra (Y2 site), and on the other side by CO_3 groups. Along [001] the decorated chains alternate their polarity. The (010) layers are stacked along [010] by hydrogen bonding (see next section).

Hydrogen bonding in lusernaite-(Y)

The calculation of the bond-valence sums (BVS) for the nine independent anion sites (Table 6) gives values significantly different from 2 valence units (*vu*) for all these sites. Examination of the O···O distances shorter than 3.0 Å (Table 7) suggests the presence of hydrogen bonds.

The undersaturation of O2 and O3 oxygen atoms, both bonded to CO_3 groups, is removed by their probable hydrogen bonding; O2 is linked to O1 (hosting an OH group), whereas O3 is bonded to O6 (hosting an OH group) and Ow1 (hosting a H_2O group). By applying the equation proposed by Ferraris & Ivaldi (1988), their BVS increase up to 1.99 and 2.01 *vu*, indicating their population by oxygen atoms. An additional O2···Ow3 hydrogen bond will be discussed below.

O1 and O6 sites, with BVS of 0.99 and 1.04 *vu*, respectively, are occupied by hydroxyl anions, as the O4 and O5 sites. Moreover, the two latter sites are not involved in any plausible hydrogen bond, and they could therefore host also fluorine atoms.

The Ow1 site is occupied by an H_2O group, which is involved in two hydrogen bonds: the Ow1···O3 bond and the Ow1···Ow1' bond, with the two Ow1 sites belonging to successive layers along [010]. The two hydrogen atoms located during the crystal structure determination, namely H1 and H2, are at 1.09 and 1.08 Å from Ow1. These bond lengths are a little longer than the expected ones, but taking into account the quality of the refinement and the possible disorder affecting the hydrogen-bond scheme, they could be retained acceptable. Owing to the presence of a mirror plane,

H1 is statistically bonded to the Ow1 of the upper or the lower layer; the H2 takes part in the Ow1-O3 bond. The H1 – Ow1 – H2 bond angle is *ca*. 98°.

A more complex situation occurs at the Ow2 and Ow3 sites. The Ow2 site is at 2.75(4) Å from Ow3. The latter has a refined electron density indicating half occupancy. Figure 4 illustrates a possible hydrogen-bonding scheme involving the Ow2 and Ow3 sites. Along [100], every two Ow2, one acts as donor in Ow2···Ow3 hydrogen bond, the other as acceptor. Consequently, the Ow2 site will be occupied, along **a**, by a regular alternation of H_2O and OH^- groups. Owing to the lack of any correlation between adjacent columns, the Ow2 site will be statistically occupied by H_2O and OH^-. In addition, Ow3 is at 2.91(4) Å from two O2 sites. The angle between O2-Ow3-Ow2 is *ca*. 114° and agrees with an hydrogen bond. It is possible that only one of the two O2 sites is involved in a hydrogen bond with Ow3. In this way, O2 could be slightly oversaturated, with a BVS of 2.13 *vu*, whereas Ow3 displays a negative BVS, *i.e*. -0.15 *vu*. The deviation from an ideal valence sum could be related to the disorder occurring along [100], with the statistically occupied Ow3 site probably representing an average position.

In conclusion, hydrogen bonds in lusernaite-(Y) are very important in assuring the link between successive (010) layers, in agreement with its perfect {010} cleavage; the hydrogen bonds linking successive layers are Ow1···Ow1 and, probably, Ow3···O2.

Crystal chemistry of lusernaite-(Y)

Crystal-structure determination and bond-valence analysis indicate that Y1 is coordinated by two oxygen anions and six hydroxyl groups, Y2 is bonded to five (OH,F) anions, two H_2O groups, and a mixed (H_2O/OH) site; Al is octahedrally coordinated by six hydroxyl groups.

Consequently, the layer of lusernaite-(Y) has a composition $Y_4Al(CO_3)_2(OH,F)_{11}\cdot 5H_2O$, being electrostatically neutral; thus the net charge of the interlayer must be zero. In fact, adjacent layers are connected through hydrogen bonding, involving also an additional water molecule, giving the actual formula of lusernaite-(Y), $Y_4Al(CO_3)_2(OH,F)_{11}\cdot 6H_2O$.

The substitution of $(Y,REE)^{3+}$ by $(Pb,Ca)^{2+}$ yields a deficit of charges, compensated through other compositional variation. Taking into account the crystal chemistry of lusernaite-(Y), the most probable mechanism could involve the Ow2 site, *i.e*. the site with the mixed occupancy by OH^- and H_2O groups. Electrostatic neutrality could be achieved through the coupled substitution

$$(Y,REE)^{3+} + {}^{Ow2}OH^- \rightarrow (Pb,Ca)^{2+} + {}^{Ow2}H_2O.$$

Other possible substitution mechanisms (*e.g*. the substitution of trivalent Y and *REE* by Pb^{2+} and a tetravalent cation) are less probable and cannot be proven.

SUMMARY AND CONCLUSION

With the discovery of lusernaite-(Y), twenty natural yttrium carbonates are known (Table 8). No yttrium carbonates without additional anions and without H_2O (group 5.A) have been described till now. Lusernaite-(Y), being a carbonate with additional anions and with H_2O, belongs to the 5.D group of Strunz & Nickel (2001). It displays a new kind of layered crystal structure, with an interlayer hosting H_2O molecules; it is also the first natural Y-Al carbonate.

Yttrium carbonates are usually found as late-stage hydrothermal phases in alkaline magmatic rocks (or their metamorphic derivatives); in some cases, they occur in the oxidation zone of U or Cu deposits. The occurrence of lusernaite-(Y) agrees with the usual genesis of these phases; in fact, it occurs in late-stage fractures as product of hydrothermal activity related to the Alpine

tectono-metamorphic events. Owing to the richness of rare minerals in the fractures of the Luserna stone, the quarries exploiting this kind of rock are an interesting field of research for the collection and the study of the crystal chemistry of yttrium and *REE* minerals.

ACKNOWLEDGEMENTS

The authors wish to thank the mineral collector Bruno Marello who provided us with the first studied specimens; additional samples, useful for the completion of the study, were provided by Giuseppe Finello and Graziano Del Core.

Andrea Risplendente (Dipartimento di Scienze della Terra "Ardito Desio", Milano, Italy) is acknowledged for his important assistance during electron-microprobe analysis. Chemical analysis of *REE* were performed using a protocol made by Valeria Diella, National Research Council, Institute of Environmental Processes. Carmelo Sibio (Dipartimento di Scienze della Terra, Torino, Italy) and Italo Campostrini (Dipartimento di Chimica Strutturale e Stereochimica Inorganica, Milano) are thanked for careful preparation of the polished crystals of lusernaite-(Y).

References

BARELLI, V. (1835): *Cenni di statistica mineralogica degli Stati di S.M. il Re di Sardegna ovvero Catalogo ragionato della raccolta formatasi presso l'Azienda Generale dell'Interno*. Fordratto, Torino, 687.

BAYLISS, P. & LEVINSON, A.A. (1988): A system of nomenclature for rare-earth mineral species: Revision and extension. *Am. Mineral.*, **73**, 422-423.

BUSSY, F. & CADOPPI, P. (1996): U-Pb dating of granitoids from the Dora-Maira massif (western Italian Alps). *Schweiz. Mineral. Petrogr. Mitt.*, **76**, 217-233.

BRESE, N.E. & O'KEEFFE, M. (1991): Bond-valence parameters for solids. *Acta Crystallogr.*, **B47**, 192-197.

CADOPPI, P. (1990): Geologia del basamento cristallino nel settore settentrionale del Massiccio Dora-Maira (Alpi Occidentali). Ph.D. Thesis, University of Torino, Italy, 201 pp.

CHAO, G.Y., MAINWARING, P.R. & BAKER, J. (1978): Donnayite, $NaCaSr_3Y(CO_3)_6{\cdot}3H_2O$, a new mineral from Mont Saint-Hilaire, Québec. *Can. Mineral.*, **16**, 335-340.

CHRISTY, A.G., GREW, E.S., MAYO, S.C., YATES, M.G. & BELAKOVSKIY, D.I. (1998): Hyalotekite, $(Ba,Pb,K)_4(Ca,Y)_2Si_8(B,Be)_2(Si,B)_2O_{28}F$, a tectosilicate related to scapolite: new structure refinement, phase transitions and a short-range ordered 3*b* superstructure. *Mineral. Mag.*, **62**, 77-92.

DE BARTOLOMEIS, L. (1847): *Notizie topografiche e statistiche sugli Stati Sardi*. Tip. Chirio e Mina, Torino, 712 pp.

DELIENS, M. & PIRET, P. (1986): La kamotoïte-(Y), un nouveau carbonate d'uranyle et de terres rares de Kamoto, Shaba, Zaïre. *Bull. Minéral.*, **109**, 643-647.

FERRARIS, G. & IVALDI, G. (1988): Bond valence *vs* bond length in O···O hydrogen bonds. *Acta Crystallogr.*, **B44**, 341-344.

FINELLO, G., AMBRINO, P., KOLITSCH, U., CIRIOTTI, M.E., BLASS, G. & BRACCO, R. (2007): I minerali della "Pietra di Luserna", Piemonte, Italia Nord-Occidentale. I. Alcune cave di gneiss della Val Luserna. *MICRO*, **2007**, 181-226.

GAFT, M., REISFELD, R. & PANCZER, G. (2005): *Modern luminescence spectroscopy of minerals and materials.* Springer, 374 pp.

GASTALDI, B. (1874): Studii geologici sulle Alpi Occidentali. Parte II. *Mem. descr. Carta Geol. It*, **2**, 3-61.

GRICE, J.D. (1996): The crystal structure of shomiokite-(Y). *Can. Mineral.*, **34**, 649-655.

GRICE, J.D. & CHAO, G.Y. (1997): Horváthite-(Y), rare-earth fluorocarbonate, a new mineral species from Mont Saint-Hilaire, Quebec. *Can. Mineral.*, **35**, 743-749.

GRICE, J.D. & GAULT, R.A. (1998): Thomasclarkite-(Y), a new sodium – rare earth-element bicarbonate. *Am. Mineral.*, **80**, 1059-1064.

GRICE, J.D., GAULT, R.A. & CHAO, G.Y. (1995): Reederite-(Y), a new sodium rare-earth carbonate mineral with a unique fluorosulfate anion. *Am. Mineral.*, **80**, 1059-1064.

GRICE, J.D., GAULT, R.A., ROBERTS, A.C. & COOPER, M.A. (2000): Adamsite-(Y), a new sodium-yttrium carbonate mineral species from Mont Saint-Hilaire, Quebec. *Can. Mineral.*, **38**, 1457-1466.

GRICE, J.D., MAISONNEUVE, V. & LEBLANC, M. (2007): Natural and synthetic fluoride carbonates. *Chem. Rev.*, **107**, 114-132.

GRICE, J.D., VAN VELTHUIZEN, J. & GAULT, R.A. (1994): Petersenite-(Ce), a new mineral from Mont Saint-Hilaire, and its structural relationship to other REE carbonates. *Can. Mineral.*, **32**, 405-414.

HOLLAND, T.J.B. & REDFERN, S.A.T. (1997): Unit cell refinement from powder diffraction data: the use of regression diagnostics. *Mineral. Mag.*, **61**, 65-77.

KHOMYAKOV, A.P., POLEZHAEVA, L.I., YAMNOVA, N.A. & PUSHCHAROVSKY, D.YU. (1992): Mineevite-(Y), $Na_{25}Ba(Y,Gd,Dy)_2(CO_3)_{11}(HCO_3)_4(SO_4)_2F_2Cl$: a new mineral. *Zap. Vses. Mineral. Obshch.*, **121**, 138-143 (in Russian).

KRAUS, W. & NOLZE, G. (1996): POWDER CELL – a program for the representation and manipulation of crystal structures and calculation of the resulting X-ray powder patterns. *J. Appl. Cryst.*, **29**, 301-303.

LI, Y., BURNS, P.C. & GAULT, R.A. (2000): A new rare-earth-element uranyl carbonate sheet in the structure of bijvoetite-(Y). *Can. Mineral.*, **38**, 153-162.

MANDARINO, J.A. (1979): The Gladstone-Dale relationship. Part III. Some general applications. *Can. Mineral.*, **17**, 71-76.

MANDARINO, J.A. (1981): The Gladstone-Dale relationship. Part IV. The compatibility concept and its application. *Can. Mineral.*, **19**, 441-450.

MILTON, C., INGRAM, B., CLARK, J.R. & DWORNIK, E.J. (1965): Mckelveyite, a new hydrous sodium barium rare-earth uranium carbonate mineral from the Green River Formation, Wyoming. *Am. Mineral.*, **50**, 593-612.

MINEEV, D.A., LAVRISHCHEVA, T.I. & BYKOVA, A.V. (1970): Yttrian bastnaesite, a product of the alteration of gagarinite. *Zap. Vses. Mineral. Obshch.*, **99**, 328-332 (in Russian).

MIYAWAKI, R., KURIYAMA, J. & NAKAI, I. (1993): The redefinition of tengerite-(Y), $Y_2(CO_3)_3 \cdot 2\text{-}3H_2O$, and its crystal structure. *Can. Mineral.*, **78**, 425-432.

MOORE, P.B., ARAKI, T. & GHOSE, S. (1982): Hyalotekite, a complex lead borosilicate: its crystal structure and the lone-pair effect of Pb(II). *Am. Mineral.*, **67**, 1012-1020.

MOORE, P.B., SEN GUPTA, P.K. & SCHLEMPER, E.O. (1985): Solid solution in plumbous potassium oxysilicate affected by interaction of a lone pair with bond pairs. *Nature*, **318**, 548.

NAGASHIMA, K., MIYAWAKI, R., TAKASE, J., NAKAI, I., SAKURAI, K., MATSUBARA, S., KATO, A. & IWANO, S. (1986): Kimuraite, $CaY_2(CO_3)_4 \cdot 6H_2O$, a new mineral from fissures in an alkali

olivine basalt from Saga Prefecture, Japan, and new data on lokkaite. *Am. Mineral.*, **71**, 1028-1033.

OTTOLINI, L., CAMARA, F. & BIGI, S. (2000) : An investigation of matrix effects in the analysis of fluorine in humite-group minerals by EPMA, SIMS, and SREF. *Am. Mineral*., **85**, 89-102.

OXFORD DIFFRACTION (2007a).*CrysAlis CCD*. Oxford Diffraction Ltd, Abingdon.

OXFORD DIFFRACTION (2007b) *CrysAlis RED*. Oxford Diffraction Ltd, Abingdon.

PEKOV, I.V., CHUKANOV, N.V., ZUBKOVA, N.V., KSENOFONTOV, D.A., HORVATH, L. ZADOV, A.E. & PUSHCHAROVSKY, D.Y. (2010): Lecoqite-(Y), $Na_3Y(CO_3)_3 \cdot 6H_2O$, a new mineral species from Mont Saint-Hilaire, Quebec, Canada. *Can. Mineral.*, **48**, 95-104.

PERTTUNEN, V. (1970): Lokkaite, a new hydrous RE-carbonate from Pyörönmaa pegmatite in Kangasala, S.W. Finland. *Bull. Geol. Soc. Finland*, **43**, 67-72.

PICCOLI, G.C., MALETTO, G., BOSIO, P. & LOMBARDO, B. (2007): *Minerali del Piemonte e della Valle d'Aosta*. Associazione Amici del Museo 'F. Eusebio', Alba, 610 pp.

RAADE, G. & BRASTAD, K. (1993): Kamphaugite-(Y), a new hydrous Ca-(Y,REE)-carbonate mineral. *Eur. J. Mineral.*, **5**, 679-683.

RAUDSEPP, M. (1995) : Recent advances in the electron-probe micro-analysis of minerals for the light elements. *Can. Mineral.*, **33**, 203-218.

SANDRONE, R. (2001): La Pietra di Luserna nella letteratura tecnico-scientifica. In *Sem. Int. "Le Pietre Ornamentali della Montagna Europea"*, Luserna San Giovanni – Torre Pellice (TO), 10-12 giugno 2001, 333-339.

SANDRONE, R., COLOMBO, A., FIORA, L., FORNARO, M., LOVERA, E., TUNESI, A. & CAVALLO, A. (2004): Contemporary natural stones from the Italian western Alps (Piedmont and Aosta Valley Regions. *Per. Mineral.*, **73**, 211-226.

SCAILLET, S., FERAUD, G., BALLEVRE, M. & AMOURIC, M. (1992): Mg/Fe and [(Mg,Fe)Si-Al_2] compositional control on argon behaviour in high-pressure white micas: A $^{40}Ar/^{39}Ar$ continuous laser-probe study from the Dora-Maira nappe of the internal western Alps, Italy. *Geochim. Cosmochim. Acta*, **56**, 2851-2872.

SHELDRICK, G.M. (2008): A short history of SHELX. *Acta Crystallographica*, **A64**, 112-122.

SOLBERG, T.N. (1982): Fluorine electron microprobe analysis: variations of X-ray peak shape. *In* Microbeam Analysis (K.F.J. Heinrich, ed.). San Francisco Press, Inc., San Francisco, California (148-150).

STRUNZ, H. & NICKEL, E.H. (2001): *Strunz Mineralogical Tables. 9th edition*. E. Schweizerbart Verlag, Stuttgart, 870 pp.

TAKAI, Y. & UEHARA, S. (2011): Hizenite-(Y), IMA 2011-030. CNMNC Newsletter No. 10, October 2011, page 2555. *Mineral. Mag.*, **75**, 2549-2561.

VACCIO, R. (2002): Cave di «Pietra di Luserna» nel territorio di Bagnolo. *In*: Piccoli, G.C., Minerali delle Alpi Marittime e Cozie. Provincia di Cuneo. Amici del Museo «F. Eusebio», Ed., Alba, 66-76.

VIALON, P. (1966): Etude géologique du Massif Dora-Maira (Alpes Cottiennes internes – Italie). *Travaux du Laboratoire Géologique de Grenoble*, **4**, 1-293.

WALLWORK, K., KOLITSCH, U., PRING, A. & NASDALA, L. (2002): Decrespignyite-(Y), a new copper yttrium rare earth carbonate chloride hydrate from Paratoo, South Australia. *Mineral. Mag.*, **66**, 181-188.

WANG, L. & ZHOU, K. (1995): The crystal structure of synchysite-(Y), $YCa(CO_3)F$. *Acta Petrol. Mineral. Sinica*, **14**, 336-344 [in Chinese with English abs.].

Table captions

Table 1 – Microprobe analyses of lusernaite-(Y): chemical composition as wt.% (average *n* = 18) and number of atoms on the basis of (O+F) = 23 *apfu*, assuming the presence of 2 (CO_3) and 6 H_2O groups *pfu*.
Table 2 – Observed X-ray powder diffraction data for lusernaite-(Y).
Table 3 – Crystal data and summary of parameters describing data collection and refinement for lusernaite-(Y).
Table 4 – Atomic coordinates and displacement parameters for lusernaite-(Y).
Table 5 – Selected bond distances (in Å) in lusernaite-(Y).
Table 6 – Bond-valence calculations for lusernaite-(Y), according to Brese & O'Keeffe (1991).
Table 7 – O···O distances (in Å) in the suggested hydrogen-bonding scheme, with corresponding bond-valence values (*vu*).
Table 8 – Comparison of natural yttrium carbonates.

Figure captions

Figure 1 – Colourless thin tabular crystals of lusernaite-(Y) associated with "chlorite". Crystal aggregate size: 2 mm. Collection and photo B. Marello.
Figure 2 – Micro-Raman spectra of lusernaite-(Y) between 200 and 1200 cm^{-1} (a) and the effect of luminescence (b) for both 473.1 and 632.8 nm excitation lines.
Figure 3 – Crystal structure of lusernaite-(Y), as seen down [100] (a) and [010] (b). Balls: red = O^{2-} or $(OH,F)^-$ anions; light blue = H_2O molecules or mixed H_2O/OH^- occupied site. Polyhedra: light blue = Y-centered polyhedra; green = Al-centered octahedra; black = CO_3 groups.
Figure 4 – The possible hydrogen bonds connecting successive (010) layers. Polyhedra: blue: Y-centered polyhedra; green: Al-centered octahedra; black = CO_3 groups. Spheres: red: O2 sites; light blue: Ow1 sites; green: Ow2 sites; yellow: Ow3 sites.

Table 1 – Microprobe analyses of lusernaite-(Y): chemical composition as wt.% (average *n* = 18) and number of atoms on the basis of (O+F) = 23 *apfu*, assuming the presence of 2 (CO_3) and 6 H_2O groups *pfu*.

Oxide	wt.% (average *n* = 18)	range	e.s.d.	*apfu* (based on 23 anions)
Al_2O_3	6.11	5.94 – 6.45	0.13	1.061
Y_2O_3	43.52	42.28 – 44.69	0.77	3.412
La_2O_3	0.02	0.00 – 0.12	0.03	0.002
Ce_2O_3	0.04	0.00 – 0.16	0.05	0.002
Nd_2O_3	0.03	0.00 – 0.12	0.03	0.002
Sm_2O_3	0.16	0.00 – 0.37	0.10	0.008
Gd_2O_3	1.39	1.06 – 1.66	0.15	0.068
Dy_2O_3	3.46	2.97 – 3.77	0.19	0.164
Er_2O_3	3.15	2.84 – 3.61	0.20	0.146
Yb_2O_3	2.09	1.75 – 2.53	0.25	0.094
CaO	0.33	0.16 – 0.58	0.12	0.052
PbO	0.37	0.19 – 0.57	0.12	0.015
F	1.40	1.19 – 1.52	0.08	0.652
H_2O*	22.74			6 H_2O 10.345 OH^-
CO_2*	9.94			1.999
Subtotal	94.75			
Les O ≡ F	-0.59			
Total	94.16			

Table 2 – Observed X-ray powder diffraction data for lusernaite-(Y).

I_{obs}	d_{meas}	I_{calc}	d_{calc}	*h k l*	I_{obs}	d_{meas}	I_{calc}	d_{calc}	*h k l*
vs	**11.02**	100	11.03	0 1 0	w	2.901	11	2.904	1 2 3
s	**7.90**	49	7.92	0 1 1	w	2.790	15	2.787	2 2 2
m	**6.41**	15	6.46	1 0 1	vw	2.667*			
m	**5.66**	25	5.69	0 0 2	vw	2.606	4	2.611	2 3 1
mw	**5.06**	24	5.06	0 1 2	w	2.526	12	2.530	0 2 4
vw	4.600*				w	2.422	9	2.426	2 3 2
mw	**4.258**	33	4.251	1 1 2	mw	2.305	11	2.304	2 0 4
w	3.961	9	3.961	0 2 2	w	2.251	5	2.256	2 1 4
vw	3.834						4	2.251	0 3 4
w	3.676	12	3.694	2 1 0	vw	2.185	1	2.182	3 2 2
		10	3.677	0 3 0	w	2.152	3	2.153	3 0 3
vw	3.592	1	3.589	0 1 3	w	2.091	5	2.097	2 4 2
w	3.504	10	3.514	2 1 1	vw	2.010	4	2.005	3 2 3
w	3.416	6	3.416	1 0 3			5	1.995	3 3 2
vw	3.345*				w	1.941	7	1.952	2 3 4
mw	**3.195**	27	3.196	2 2 0	w	1.824	4	1.822	2 5 2
mw	**3.095**	21	3.099	2 1 2	w	1.711	5	1.708	2 0 6

***Notes**: the d_{hkl} values were calculated on the basis of the unit-cell refined by using single-crystal data. Intensities (I/I_{100} > 1 only) were calculated on the basis of the structural model. Observed intensities were visually estimated. vs = very strong; s = strong; ms = medium-strong; m = medium; mw = medium-weak; w = weak; vw = very weak.The * indicates three unindexed reflections, probably due to unidentified impurities.*

Table 3 – Crystal data and summary of parameters describing data collection and refinement for lusernaite-(Y).

Crystal data	
Crystal size (mm^3)	0.33 x 0.09 x 0.01
Cell setting, space group	Orthorhombic, *Pmna*
Unit-cell dimensions	
a (Å)	7.8412(3)
b (Å)	11.0313(5)
c (Å)	11.3870(4)
V ($Å^3$)	984.96(7)
Z	2
Data collection and refinement	
Radiation type, (λ)	Mo *K*α (0.71073 Å)
Temperature (K)	~ 298
Maximum observed 2θ(°)	52.74
Measured reflections	23367
Unique reflections	1081
Reflections $F_o > 4\sigma F_o$	840
R_{int}	0.1131
$R\sigma$	0.0475
Range of *h*, *k*, *l*	$-9 \le h \le 9$ $-13 \le k \le 13$ $-14 \le l \le 14$
R_1 [$F_o > 4\sigma F_o$]	0.0681
R_1 (all data)	0.0861
wR_2 (on F_o^2)	0.1993
Goof	1.055
Number of l.s. parameters	89
$\Delta\rho_{max}$ and $\Delta\rho_{min}$	2.67, −1.09

Table 4 – Atomic coordinates and displacement parameters for lusernaite-(Y).

Site	*x/a*	*y/b*	*z/c*	U_{11}	U_{22}	U_{33}	U_{23}	U_{13}	U_{12}	$U_{eq/iso}$
Y1	¼	0.4975(2)	¾	0.0119(7)	0.0281(13)	0.0111(7)	0	0.0007(4)	0	0.0170(6)
Pb1a	¼	0.570(7)	¾	0.0119(7)	0.0281(13)	0.0111(7)	0	0.0007(4)	0	0.0170(6)
Pb1b	¼	0.409(5)	¾	0.0119(7)	0.0281(13)	0.0111(7)	0	0.0007(4)	0	0.0170(6)
Y2	0	0.2304(1)	0.8487(1)	0.0166(8)	0.0282(9)	0.0160(8)	0.0001(6)	0	0	0.0203(6)
Al	0	½	0	0.012(3)	0.034(4)	0.009(3)	- 0.002(2)	0	0	0.0182(16)
C	½	0.683(1)	0.915(1)	0.016(8)	0.036(9)	0.012(7)	0.007(6)	0	0	0.0213(34)
O1	-0.1624(9)	0.3949(7)	0.9272(6)	0.010(4)	0.046(5)	0.013(4)	- 0.001(3)	0.001(3)	0.001(3)	0.0233(19)
O2	0.357(1)	0.6424(8)	0.8745(7)	0.017(4)	0.054(6)	0.030(5)	- 0.009(4)	0.007(3)	- 0.007(4)	0.0338(23)
O3	½	0.759(1)	0.9988(9)	0.022(6)	0.038(6)	0.018(5)	- 0.011(4)	0	0	0.0258(26)
O4	- ¼	0.213(1)	¾	0.016(5)	0.046(7)	0.020(5)	0	0.000(3)	0	0.0273(26)
O5	0	0.4177(9)	0.1437(8)	0.021(6)	0.033(6)	0.006(5)	0.007(4)	0	0	0.0199(24)
O6	0	0.387(1)	0.7091(9)	0.019(6)	0.037(7)	0.007(5)	0.007(4)	0	0	0.0214(25)
Ow1	-0.188(2)	0.135(1)	0.9854(9)	0.052(7)	0.062(7)	0.050(7)	0.019(5)	0.016(5)	0.007(6)	0.0548(30)
Ow2	0	0.033(2)	0.770(2)	0.091(17)	0.103(16)	0.087(16)	- 0.036(12)	0	0	0.0936(71)
Ow3	- ¼	- 0.141(4)	¾							0.101(15)
H1	- 0.201	0.037	0.989							0.05
H2	- 0.314	0.158	0.014							0.05

Table 5 – Selected bond distances (Å) for lusernaite-(Y).

Y1	– O2	2.297(8) × 2	Y2	– O4	2.267(1) × 2
	– O6	2.353(6) × 2		– O6	2.350(10)
	– O1	2.413(7) × 2		– Ow2	2.354(21)
	– O5	2.486(6) × 2		– Ow1	2.387(10) × 2
<Y1–O>		2.387		– O1	2.391(7) × 2
			<Y2–O>		2.351
Al	– O5	1.872(9) × 2	C	– O3	1.268(19)
	– O1	1.912(7) × 4		– O2	1.290(11) × 2
<Al–O>		1.899	<C–O>		1.28
			O2 – C – O3		119.9(7)°
			O2 – C – O2		120.2(5)°

Table 6 – Bond-valence calculations for lusernaite-(Y), according to Brese & O'Keeffe (1991).

	Y1	Y2	Al	C	Σν (O-X)	Σν (O-X)*	species
O1	0.34[a]	0.36[a]	0.49[b]		1.19	0.99	OH^-
O2	0.47[a]			1.31[a]	1.78	1.98 2.13**	O^{2-}
O3				1.39	1.39	1.99	O^{2-}
O4		0.46[a]			0.92	0.92	OH^-,F^-
O5	0.28[a]		0.55[a]		1.11	1.11	OH^-
O6	0.40[a]	0.40			1.20	1.04	OH^-
Ow1		0.36[a]			0.36	0.01*** 0.27****	H_2O
Ow2		0.40			0.40	0.20 0.60	H_2O OH^-
Ow3					0.00	-0.15	H_2O
Σν (X-O)	2.98	3.16	3.06	4.01			

[a](2 X →). [b] (4 X →). *Bond valence after correction for O···O hydrogen bonds. **If involved in Ow3···O2 hydrogen bond. ***If donor in Ow1···Ow1 hydrogen bond. ***If acceptor in Ow1···Ow1 hydrogen bond. For Y1 and Y2 sites, the parameters for Y-O and Y-F bonds were used.

Table 7 – O···O distances (in Å) in the suggested hydrogen-bonding scheme, with corresponding bond-valence values (*vu*).

O···O bond donor → acceptor	d (Å)	*vu*
Ow1 (H_2O) → O3 (O)	2.72(1)	0.22
Ow2 (H_2O/OH) ↔ Ow3 (H_2O)	2.75(4)	0.20
O1 (OH) → O2 (O)	2.76(1)	0.20
O6 (OH) → O3 (O)	2.89(2)	0.16
Ow3 (H_2O) → O2(O)	2.91(4)	0.15
Ow1 (H_2O) ↔ Ow1 (H_2O)	2.99(2)	0.13

Table 8 – Comparison of natural yttrium carbonates.

	Chemical formula	*a* (Å)	*b* (Å)	*c* (Å)	α (°)	β (°)	γ (°)	S.G.	Ref.
5.B Carbonates with additional anions, without H_2O									
bastnäsite-(Y)	$(Y,REE)(CO_3)F$	6.57	6.57	9.48	90	90	120	*P*6	[1]
horváthite-(Y)	$NaY(CO_3)F$	6.96	9.17	6.30	90	90	90	*Pmcn*	[2]
mineevite-(Y)	$Na_{25}Ba(Y,Gd,Dy)_2(CO_3)_{11}(HCO_3)_4(SO_4)F_2Cl$	8.81	8.81	37.03	90	90	120	$P6_3/m$	[3]
reederite-(Y)	$Na_{15}Y_2(CO_3)_9(SO_3F)Cl$	8.77	8.77	10.75	90	90	120	*P*-6	[4]
synchysite-(Y)	$Ca(Y,Ce)(CO_3)_2F$	12.04	6.95	18.44	90	102.45	90	*C*2/*c*	[5]
5.C Carbonates without additional anions, with H_2O									
adamsite-(Y)	$NaY(CO_3)_2{\cdot}6H_2O$	6.26	13.05	13.22	91.17	103.70	89.99	*P*-1	[6]
donnayite-(Y)	$NaCaSr_3Y(CO_3)_6{\cdot}3H_2O$	9.00	9.00	6.79	102.77	116.28	59.99	*P*1	[7]
hizenite-(Y)	$Ca_2Y_6(CO_3)_{11}{\cdot}14H_2O$	6.30	9.09	63.49	90	90	90	UK	[8]
kimuraite-(Y)	$CaY_2(CO_3)_4{\cdot}6H_2O$	9.25	23.98	6.04	90	90	90	*Imm*2 *Immm* *I*222 $I2_12_12_1$	[9]
lecoqite-(Y)	$Na_3Y(CO_3)_3{\cdot}6H_2O$	11.32	11.32	5.93	90	90	120	$P6_3$	[10]
lokkaite-(Y)	$CaY_4(CO_3)_7{\cdot}9H_2O$	39.07	6.08	9.19	90	90	90	*Pb*2*m* *Pbm*2 *Pbmm*	[11]
mckelveyite-(Y)	$NaCa(Ba,Sr)_3(Y,REE)(CO_3)_6{\cdot}3H_2O$	9.17	9.17	9.15	90	90	90	*P*-3	[12]
shomiokite-(Y)	$Na_3Y(CO_3)_3{\cdot}3H_2O$	10.04	17.32	5.94	90	90	90	$Pbn2_1$	[13]
tengerite-(Y)	$Y_2(CO_3)_3{\cdot}2\text{-}3H_2O$	6.08	9.16	15.11	90	90	90	$Bb2_1m$	[14]
5.D Carbonates with additional anions, with H_2O									
decrespignyite-(Y)	$(Y,REE)_4Cu(CO_3)_4Cl(OH)_5{\cdot}2H_2O$	8.90	22.77	8.59	90	120.06	90	*P*2 *Pm* *P*2/*m*	[15]
kamphaugite-(Y)	$Ca(Y,REE)(CO_3)_2(OH){\cdot}H_2O$	7.43	7.43	21.79	90	90	90	$P4_12_12$	[16]
lusernaite-(Y)	$Y_4Al(CO_3)_2(OH,F)_{11}{\cdot}6H_2O$	7.84	11.03	11.39	90	90	90	*Pmna*	[17]
thomasclarkite-(Y)	(Na,Ce)(Y,REE)(HCO_3)(OH)3·4H2O	4.56	13.02	4.56	90	90.15	90	*P*2	[18]
5.E Uranyl carbonates									
bijvoetite-(Y)	$(Y,Dy)_2(UO_2)_4(CO_3)_4(OH)_6{\cdot}11H_2O$	21.23	12.96	44.91	90	90	90	$B2_1$	[19]
kamotoite-(Y)	$Y_2U_4(CO_3)_3O_{12}{\cdot}14.5H_2O$	21.22	12.93	12.39	90	115.3	90	$P2_1/n$	[20]

[1] Mineev *et al*., 1970; [2] Grice & Chao, 1997; [3] Khomyakov *et al*., 1992; [4] Grice *et al*., 1995; [5] Wang & Zhou, 1995; [6] Grice *et al*., 2000; [7] Chao *et al*., 1978; [8] Takai & Uehara, 2011; [9] Nagashima *et al*., 1986; [10] Pekov *et al*., 2010; [11] Perttunen, 1970; [12] Milton *et al*., 1965; [13] Grice, 1996; [14] Miyawaki *et al*., 1993; [15] Wallwork *et al*., 2002; [16] Raade & Brastad, 1993; [17] this work; [18] Grice & Gault, 1998; [19] Li *et al*., 2000; [20] Deliens & Piret, 1986.

Figure 1 – Colourless thin tabular crystals of lusernaite-(Y) associated with "chlorite". Crystal aggregate size: 2 mm. Collection and photo B. Marello.

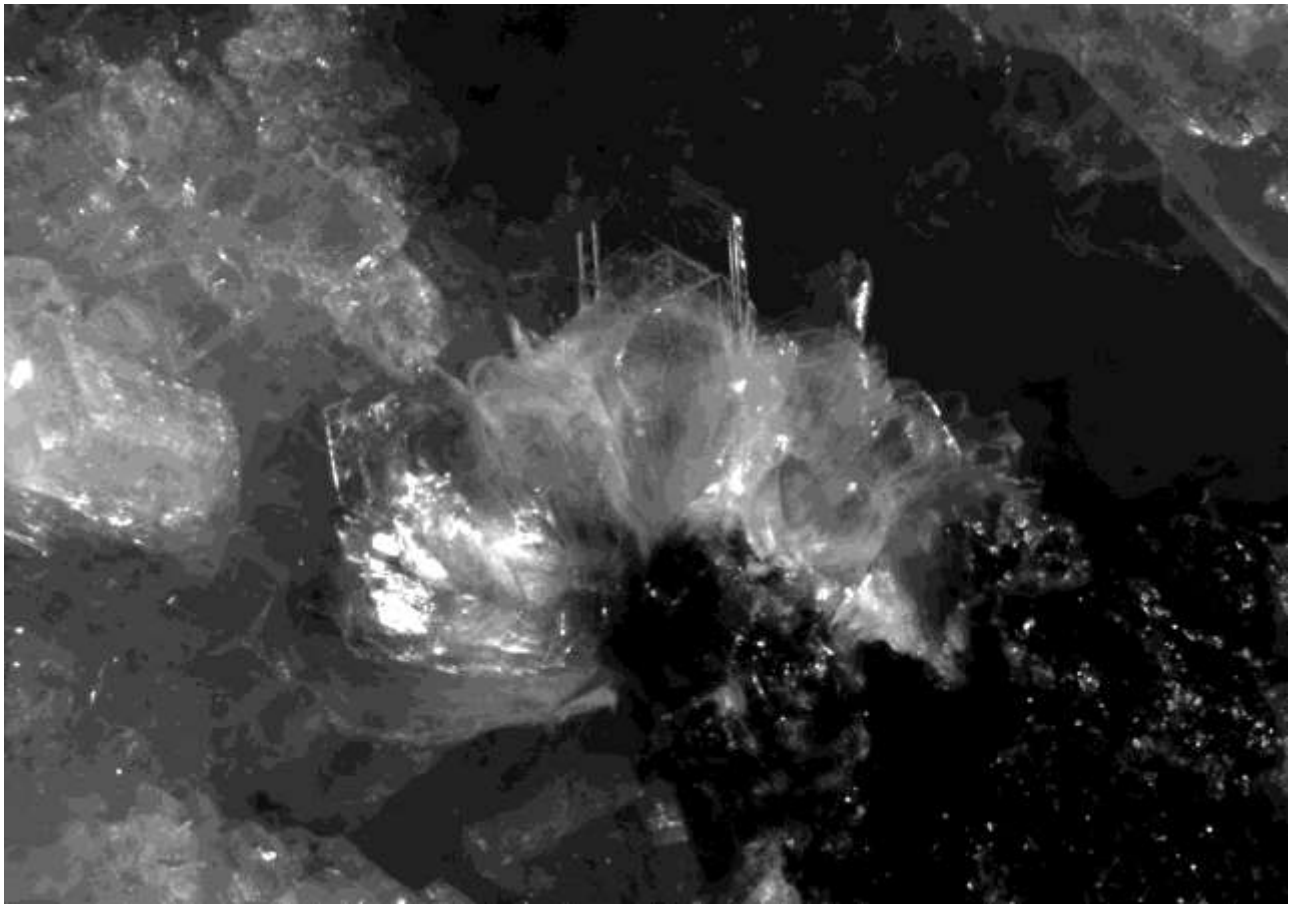

Figure 2 – Micro-Raman spectra of lusernaite-(Y) between 200 and 1200 cm^{-1} (a) and the effect of luminescence (b) for both 473.1 and 632.8 nm excitation lines.

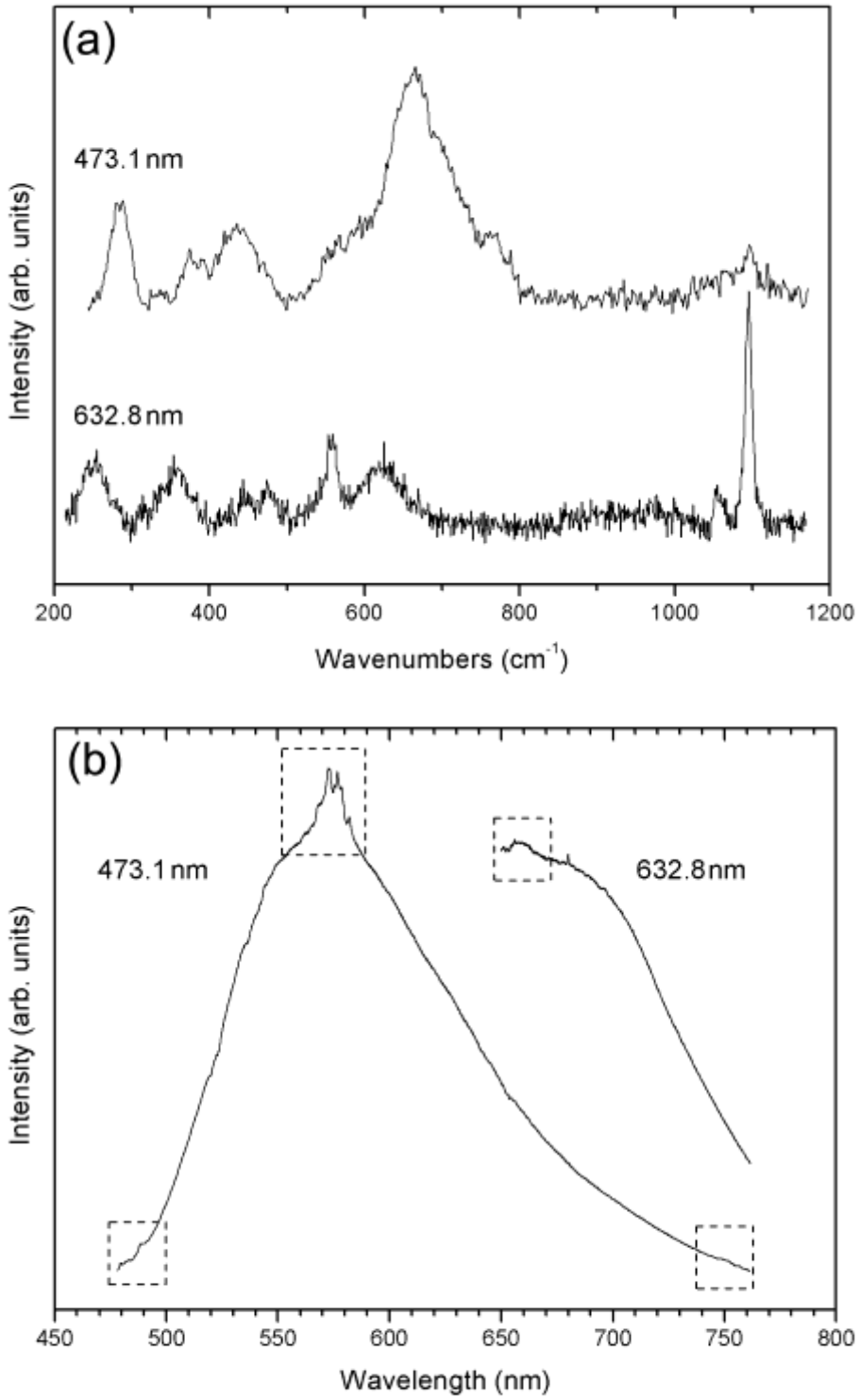

Figure 3 – Crystal structure of lusernaite-(Y), as seen down [100] (a) and [010] (b). Polyhedra: dark grey = Y-centered polyhedra; light grey = Al-centered octahedra; black = CO_3 groups. Balls: dark grey = O^{2-} or $(OH,F)^-$ anions; light grey = H_2O molecules or mixed H_2O/OH^- occupied site.

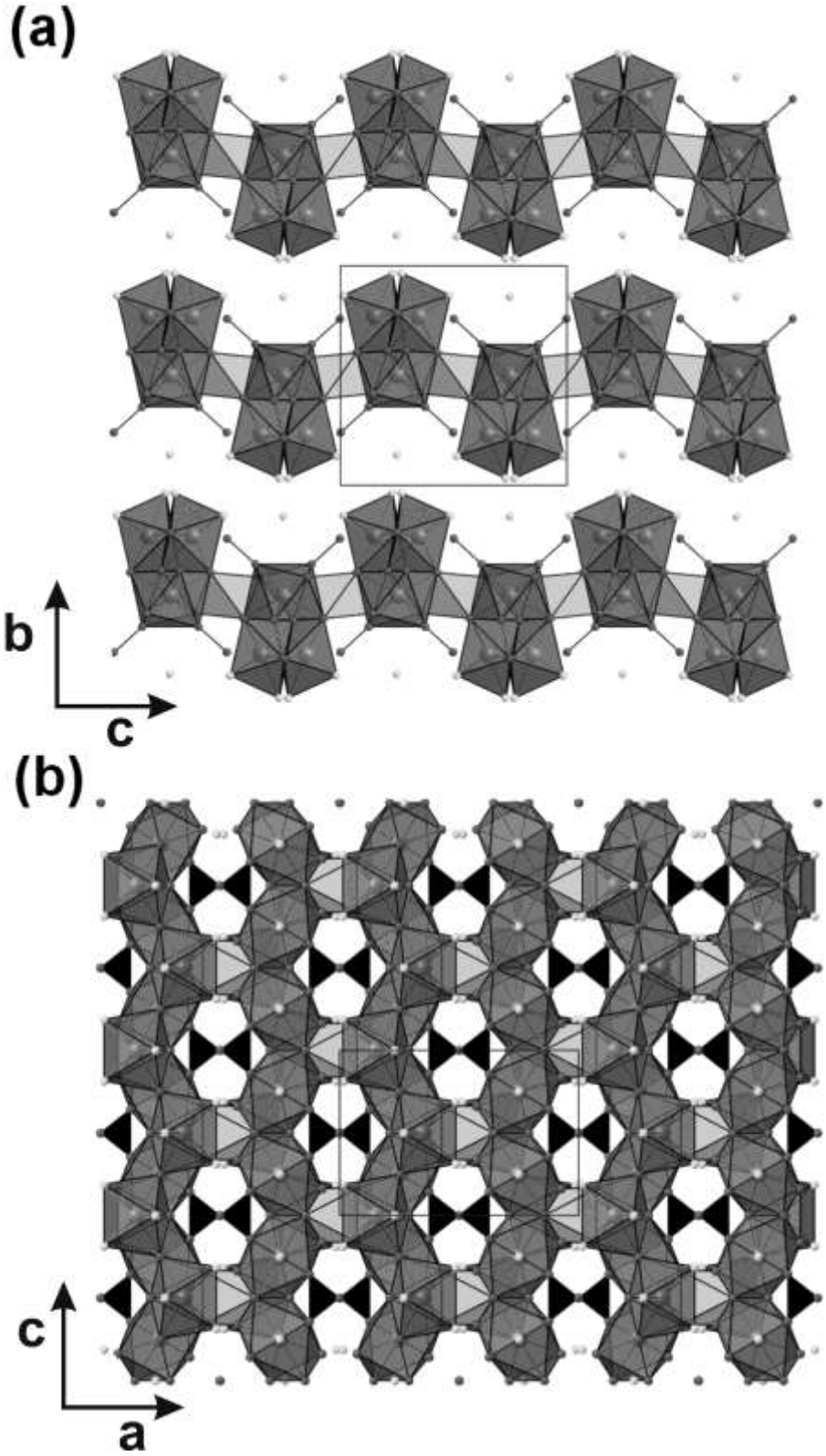

Figure 4 – The possible hydrogen bonds connecting successive (010) layers. Polyhedra: dark grey: Y-centered polyhedra; light grey: Al-centered octahedra; black = CO_3 groups. Balls: dark grey: O2 sites; grey: Ow1, Ow2, Ow3 sites.